Journal of Molecular Catalysis A: Chemical 420 (2016) 294–302

Contents lists available at ScienceDirect

Journal of Molecular Catalysis A: Chemical

journal homepage: www.elsevier.com/locate/molcata

Tungstophosphoric acid supported on core-shell polystyrene-silica microspheres or hollow silica spheres catalyzed trisubstituted imidazole synthesis by multicomponent reaction

Marina Gorsd, Gabriel Sathicq, G. Romanelli, L. Pizzio*, M. Blanco

Centro de Investigación y Desarrollo en Ciencias Aplicadas "Dr. J.J Ronco" (CINDECA), Departamento de Química, Facultad de Ciencias Exactas, UNLP-CCT La Plata, CONICET, 47 N° 257, 1900 La Plata, Argentina

ARTICLE INFO

Article history:
Received 17 February 2016
Received in revised form 8 April 2016
Accepted 12 April 2016
Available online 5 May 2016

Keywords:
Hollow silica spheres
Polystyrene-silica spheres
Tungstophosphoric acid
Trisubstituted imidazoles

ABSTRACT

Materials based on tungstophosphoric acid supported on core-shell polystyrene-silica microspheres or hollow silica spheres were prepared, characterized and used as catalysts in the synthesis of trisubstituted imidazoles by a multicomponent reaction under solvent-free conditions.

For the preparation of the two different silica-based structures, silica was synthesized using tetraethylorthosilicate (TEOS) as precursor in an ethanol-ammonium solution and polystyrene spheres as template or core. The formation and growth of the silica layer to obtain the core-shell microspheres were followed by 24 h. Then, the hollow spheres were obtained by calcination of the core-shell material at 500 °C for 3 h. Both supports were impregnated with tungstophosphoric acid (TPA) solutions.

A smooth appearance of the spheres was observed by scanning electron microscopy (SEM). Mesoporous materials were obtained, without important microporosity, as determined from N_2 adsorption-desorption isotherms. The Fourier transform infrared (FT-IR) spectra confirmed that complete removal of the polystyrene core can directly be achieved by calcination at 500 °C, and also that Keggin undegraded TPA species are present in the impregnated solids. The acidic characteristics of the solids were evaluated by potentiometric titration, showing that they exhibit very strong acid sites. Moreover, peaks assigned to crystalline forms of TPA were observed by XRD.

The yields obtained in the solvent-free synthesis of 2,4,5-triphenyl-1*H*-imidazole and other eight trisubstituted imidazoles were high, without formation of by-products resulting from competitive reactions or decomposition products, so the prepared materials are highly selective catalysts.

1. Introduction

Recently, numerous important heterocyclic compounds have been synthesized under solvent-free conditions by a multicomponent reaction [1,2]. Compounds containing imidazole moiety have many pharmacological properties and play important roles in biochemical processes [3]. Various applications have been reported in the therapeutic area, including anti-inflammatory, antiviral, antibacterial, antiallergenic and antitumor activity [4–6]. Also, imidazole moiety acts as a central section of biological systems such as Losartan and Olmesartan, which are antihypertensive. A variety of heterocyclic derivatives of this system were used as inhibitor of heme 1-oxygenase, HMG-CoA reductase, P2X7 receptors [7], and p38 MAP kinase [8].

In addition, imidazole-containing compounds play a key role in green chemistry and catalysis. Many commercial ionic liquids are based on imidazoles, due to the easy functionalization of the imidazole ring and the ability to form cations. A variety of ionic liquids were prepared, and their activity was investigated in catalytic reactions [9,10].

In 1882, Radziszewski [11], and Japp and Robinson [12] reported the first synthesis of the highly substituted imidazoles from a 1,2-dicarbonyl compound, different aldehydes, and ammonia. The preparation of heterocyclic compounds typically involves a large number of processes that use toxic reagents and generate toxic waste. A conventional preparation of trisubstituted imidazoles is performed by condensing a 1,2-diketone, an aldehyde and ammonium acetate in the presence of strong acids, such as H_3PO_4, H_2SO_4 and CH_3COONH_4 [13]. Today, there are a variety of methods for

* Corresponding author.
E-mail addresses: lrpizzio@quimica.unlp.edu.ar, lrpizzio@hotmail.com (L. Pizzio).

http://dx.doi.org/10.1016/j.molcata.2016.04.010
1381-1169/

the synthesis of substituted imidazoles, but many of these methods have disadvantages, such as low yields, long reaction times, extreme reaction conditions, use of expensive and toxic catalysts, and they often require a further reaction step for the synthesis of the desired compound.

These factors result in the need to develop alternatives for the production of substituted imidazoles in order to remove hazardous solvents and catalysts. The use of multicomponent reactions, heterogeneous catalysts and solvent-free reaction conditions would be the methodology to overcome these limitations [14–16].

On the other hand, hollow spheres and core-shell mesoporous structures have attracted increasing attention in recent years because they have an important field of application in different scientific scopes, such as catalysis [17–19], delivery of drugs [20] and medicinal use [21].

The most common method of preparation of core-shell spheres is the deposition of the desired material on a template or the use of specific functional groups on the surface of the template employed as core to induce the formation of the shell, and thus obtain a core-shell shaped structure. Then, if the material to be obtained must be hollow, the core or template is removed by calcination and/or extraction with an organic solvent depending on the system composition, though the variety of methods to prepare hollow spherical materials is diverse. Hard polymers [22], carbon spheres [23,24], silica microspheres [25], colloidal nanoparticles [26], oil/water (O/W) or water/oil (W/O) emulsion drops [27,28], or gas bubbles [29] have been used as template for the preparation of these materials. The hollow inside these materials can be used as a "microreactor", in which the chemical reactions occur differently than at the macroscale due to the effects caused by the microenvironment [30]. They also have interesting properties, such as uniform pore size, high surface area, large void space, and good biocompatibility.

In the present work, the catalytic activity of a catalyst with Keggin structure, which was confined both in silica microspheres with core-shell structure and hollow silica microspheres, was evaluated in the synthesis of imidazole. The method used to obtain the catalytic materials gave good results. Polystyrene spheres were used as core or template. On this polymer, a silica layer was deposited to form a shell by the Stöber approach. This is a well-known and efficient process to obtain uniform spherical colloidal silica particles via the hydrolysis and condensation of tetraethoxysilane (TEOS) in ethanol aqueous solution [31] by the sol-gel technique. In addition, in order to obtain the hollow microspheres, the template was removed by thermally treating the solids at high temperatures or by extraction with suitable solvents, as reported in the literature [32,33]. After the physicochemical characterization of the solids, their catalytic behavior in 2,4,5-triphenyl-1*H*-imidazole synthesis was firstly evaluated, and then the best catalyst was used to perform the synthesis of 2-(4-nitrophenyl)-4,5-diphenyl-1*H*-imidazole, 2-(4-methoxyphenyl)-4,5-diphenyl-1*H*-imidazole, and 2-(4-chlorophenyl)-4,5-diphenyl-1*H*-imidazole, which was carried out under solvent-free conditions in a multicomponent reaction, in order to achieve a method with low environmental impact.

2. Experimental

2.1. Preparation of polystyrene/silica spheres with core-shell structure

Monodisperse polystyrene (PS) spheres were synthesized employing the best conditions found in previous work [34]. They were prepared from 10 g of styrene (Aldrich, >99%) using 4,4′ azobis 4-cyanovaleric acid (ACVA) (Aldrich, >98%) as polymerization initiators, in the presence of 0.3 g of polyvinyl pyrrolidone (PVP) (Aldrich, PM = 29000) as surfactant agent.

To obtain the silica coating, PS templates in a quantity of 60% w/w with respect to the silica quantity to be prepared were weighed and placed in 40 cm^3 of ethanol, and then were sonicated for 10 min, in order to obtain a homogeneous dispersion. The modified Stöber method [35] was used for silica synthesis, which proceeds via hydrolysis/condensation of tetraethylorthosilicate (TEOS) in an alcohol/ammonium hydroxide reaction medium. Seven cm^3 of TEOS as silica precursor and 1 cm^3 of ammonium hydroxide (28% w/w) as catalyst of the sol-gel reaction were employed. The condensation reaction was performed at 50 °C with constant stirring for 20 h.

After this time, the coated spheres were separated by centrifugation and repeatedly washed with distilled water to remove the catalyst remains. Finally, they were dried at room temperature and then placed in a stove at 60 °C for 24 h, thus obtaining the solids that will be named PS@Si.

2.2. Preparation of hollow silica spheres

Part of the core-shell spheres reported in the previous section were calcined at 500 °C using a heating rate of 50 °C every 25 min in order to obtain the hollow silica spheres; the sample will be named @SiT500.

2.3. Impregnation of core-shell spheres and hollow silica spheres with tungstophosphoric acid

By employing the incipient wetness impregnation technique and using a solution of tungstophosphoric acid ($H_3PW_{12}O_{40}{\cdot}23H_2O$) (TPA) in ethanol-water (1:1 (v/v)), the following materials were impregnated: polystyrene spheres coated with silica (PS@Si) and hollow silica spheres (@SiT500). The quantity of TPA solution was fixed in order to obtain 30% and 60% of TPA (w/w) in the final material. The system was kept at room temperature till entire dryness. Afterward, the obtained solids (PS@SiTPA30, PS@SiTPA60, @SiT500TPA30 and @SiT500TPA60) were weighed. Then, the solids with core-shell structure were calcined at 200 °C to obtain the materials PS@SiTPA30T200 and PS@SiTPA60T200.

2.4. Characterization of supports and catalysts

The morphological study of the solids was performed by means of scanning electron microscopy (SEM), using Philips equipment, model 505, at a working potential of 15 kV. The samples were supported on graphite and metallized with a sputtered gold film before the measurement.

The Fourier transform infrared (FT-IR) spectra of the solids were recorded with Bruker IFS 66 equipment. Pellets of ca. 1% (w/w) of the sample in KBr were prepared in a self-made device. A wavenumber range of 400–4000 cm^{-1} was studied, the resolution being 2 cm^{-1}.

The specific surface area, the pore volume and the mean pore diameter of the solids were determined from the N_2 adsorption-desorption isotherms at liquid-nitrogen temperature, obtained by employing Micromeritics Accusorb 2100E equipment. The solids were previously degassed at 100 °C for 2 h.

Potentiometric titration was used to evaluate the acidic characteristics of the solids. To this end, 50 mg of solid suspended in 45 cm^3 of acetonitrile was stirred for 3 h. Then, the titration was carried out with a solution of *n*-butylamine in acetonitrile (0.05 N) at a flow rate of 0.05 cm^3/min. The electrode potential variation was measured in a Hanna 211 digital pH meter with a double-junction electrode.

The X-ray diffraction (XRD) patterns were obtained by the Debye-Scherrer method (powder method). The patterns were

recorded using Philips PW-1732 equipment with a built-in recorder. The conditions used were: Cu Kα radiation, Ni filter, 20 mA and 40 kV in the high voltage source, scanning range from 5 to 60 2θ, and a scanning speed of 1°/min.

2.5. Synthesis of trisubstituted imidazoles

Firstly, the synthesis of 2,4,5-triphenyl-1*H*-imidazole was studied. The reactions were carried out in a batch reactor, which was immersed in an oil bath with temperature control using a benzyl:benzaldehyde:ammonium acetate molar ratio of 1:1:1.2 and 1% mmol of catalyst, in the absence of solvent. The mixture was heated up to 130 °C for 90 min. The optimal operating conditions were previously obtained following the guidelines of the work of Raffie et al. [36], in which a Wells-Dawson heteropolyacid was used as acid catalyst.

After the reaction time was reached, the obtained solid was washed twice with 2 cm^3 of distilled water, and the solvent was evaporated in a vacuum oven to concentrate the reaction mixture up to constant weight at room temperature. Then, product separation was performed by means of three extractions with 2 cm^3 of solvent, leaving the catalyst as a solid phase, which was then dried at 40 °C in a vacuum oven.

The organic extracts were dried and concentrated in a vacuum oven at room temperature. The residue was purified by recrystallization using ethanol as the recrystallization solvent. The percentage yield for each case was calculated as the percentage of the product/reactive molar ratio.

The product obtained was identified by ^1H and ^{13}C nuclear magnetic resonance (NMR) spectroscopy. ^1H and ^{13}C NMR spectra were recorded on a Bruker Avance II 500 at 500.13 and 125.77 MHz, respectively, in DMSO-*d*6, unless indicated otherwise. Chemical shifts are given in ppm downfield from TMS as internal standard, and J values are given in Hz.

The catalyst that gave the better yield in 2,4,5-triphenyl-1*H*-imidazole synthesis was selected to prepare other eight trisubstituted imidazoles, following the same procedure described above, under the same reaction conditions, and using the corresponding aldehyde in each case.

2.6. Catalyst reuse

Stability tests of the bulk or silica-supported acid catalysts were carried out by running four consecutive experiments, under the same reaction conditions. After each test, the catalyst was separated from the reaction mixture by filtration, washed with solvent (2×2 cm^3), dried under vacuum, and then reused.

3. Results and discussion

3.1. Material characterization

The prepared materials were firstly characterized by SEM. The micrographs of the PS@Si, PS@SiTPA30, PS@SiTPA30T200, @SiT500 and @SiT500TPA30 samples are shown in Figs. 1 and 2. In all the cases, the microspheres presented a uniform appearance without formation of silica aggregates. The absence of isolated silica is due to a previous optimization of the conditions needed to obtain the coating [37].

As shown in the micrographs of the PS spheres covered with silica (Fig. 1a) and those of the PS spheres covered with silica impregnated with tungstophosphoric acid both dried and calcined at 200 °C (Fig. 1b and c, respectively), the silica shell has not only a smooth appearance, but also the same morphology after the impregnation and calcination processes. Similar images were obtained for the PS@SiTPA60 and PS@SiTPA60T200 samples.

On the other hand, the micrographs of both the hollow silica spheres and those impregnated with tungstophosphoric acid are presented in Fig. 2. It is observed that they have similar characteristics to those of the previous solids. The treatment employed to remove the PS template in a slow and controlled manner allowed avoiding possible cracks in the material. This procedure has the advantages of lower cost and time compared to the extraction of the core using organic solvents, which was reported in previous studies [34]. Though the micrograph corresponding to the material with the lower content is presented, that of the solid with higher concentration (60% TPA (w/w)) showed similar features.

The characterization by FT-IR showed that the characteristic bands of polystyrene at 3025, 2929, 2849, 1601, 1492, 1459, 1027, 906, 747 and 694 cm^{-1} [38] appear in the spectra of both the PS@Si material and those obtained by its impregnation with tungstophosphoric acid (Fig. 3a).

In addition, the characteristic bands of silica with maxima at 1094, 962 and 800 cm^{-1} (assigned to the stretching vibration of the Si–O–Si and Si–O groups) and the band at 465 cm^{-1} (ascribed to the torsion vibration of the Si–O group) are present in the spectra, and they agree well with those reported in the literature [39].

In order to plainly observe the bands assigned to TPA, the FT-IR spectra of the same solids in a wavenumber scale between 1200 and 400 cm^{-1} are presented in Fig. 3b, where the bands corresponding to the undegraded tungstophosphate anion ($[PW_{12}O_{40}]^{3-}$) can be more clearly noted. The band assigned to the vibration of the P–Oa group bond, characteristic of the TPA anion, appears at 1080 cm^{-1}, well defined though overlapped with a band attributed to SiO_2, and the band at 796 cm^{-1}, assigned to the W–Oc–W group, is observed as a transmittance increase of a support band. However, the bands corresponding to the vibration of the W–Od and W–Ob–W groups are clearly displayed at 981 cm^{-1} and 894 cm^{-1}, respectively, without overlapping. All the observed bands are consistent with those reported in the literature [40]. It must be remarked that Oa indicates the oxygen bridging W placed in the four triads of the octahedra and the P heteroatom of the central tetrahedron; Ob corresponds to the oxygen linking the triads through corners; Oc is the edge sharing oxygen, and Od denotes terminal oxygen [41].

The spectra corresponding to the PS@SiTPA60 and PS@SiTPA60T200 samples are presented in Fig. 4. The characteristic bands of PS, silica and the groups assigned to the tungstophosphate anion indicated previously were observed. No significant differences were noted between the material with and without calcination at 200 °C.

In the FT-IR spectrum of the hollow spheres (@SiT500 sample), the bands assigned to the stretching vibrations of the Si–O–Si and Si–O groups are observed (Fig. 5) and correlate well with those reported in the literature [42]. It is noteworthy that the main characteristic bands of PS are not evident in the spectrum, indicating a complete removal of the polymer after the thermal treatment at 500 °C.

With regard to the TPA-impregnated hollow silica spheres, as observed for the @SiT500TPA30 solid in Fig. 5, the bands with maxima at 1080, 981, 894, and 796 cm^{-1}, attributed to the stretching vibrations of the TPA anion, behaved in a similar manner, as explained before for the core-shell solids. The first band is overlapped with a SiO_2 band, the second band is observed as a transmittance increase of a SiO_2 band, and the other two bands are well defined. Thus, it can be concluded that the undegraded Keggin anion is present.

The textural properties of the different solids prepared were determined through the N_2 adsorption-desorption isotherms at liquid N_2 temperature. The specific surface area (S_{BET}) of the materials, together with the mean pore diameter (Dp), estimated from the BET surface, and the total pore volume (Vp), estimated from the value corresponding to a $p/p_0 = 0.98$ ratio, as well as the specific microp-

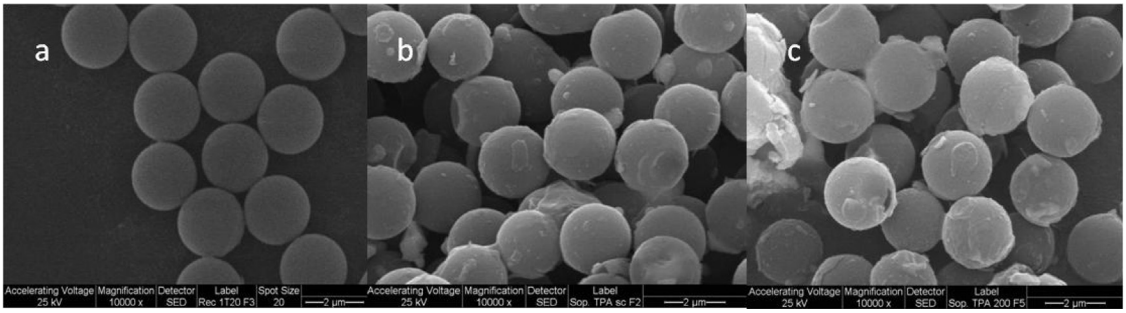

Fig. 1. SEM micrographs of (a) polystyrene spheres covered with silica, (b) silica-covered spheres impregnated with TPA, (c) silica-covered spheres impregnated with TPA after calcination at 200 °C. Magnification: 10,000×, bar: 2 µm.

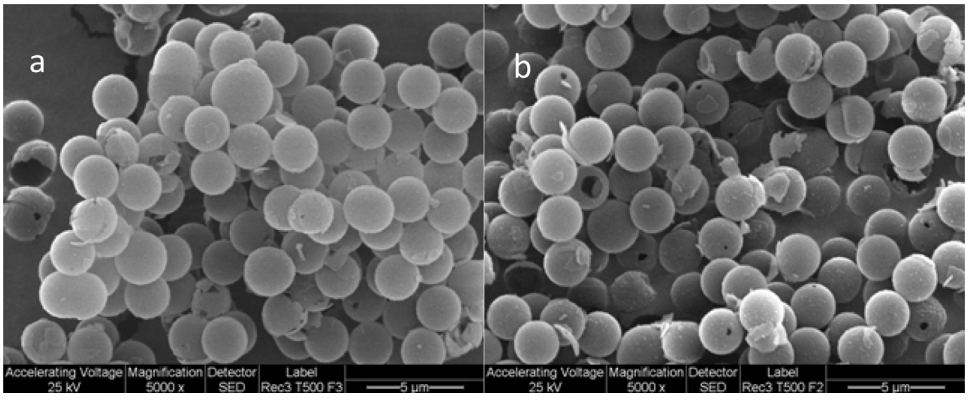

Fig. 2. SEM micrographs of (a) hollow silica spheres, (b) hollow silica spheres impregnated with TPA. Magnification: 5000×, bar: 5 µm.

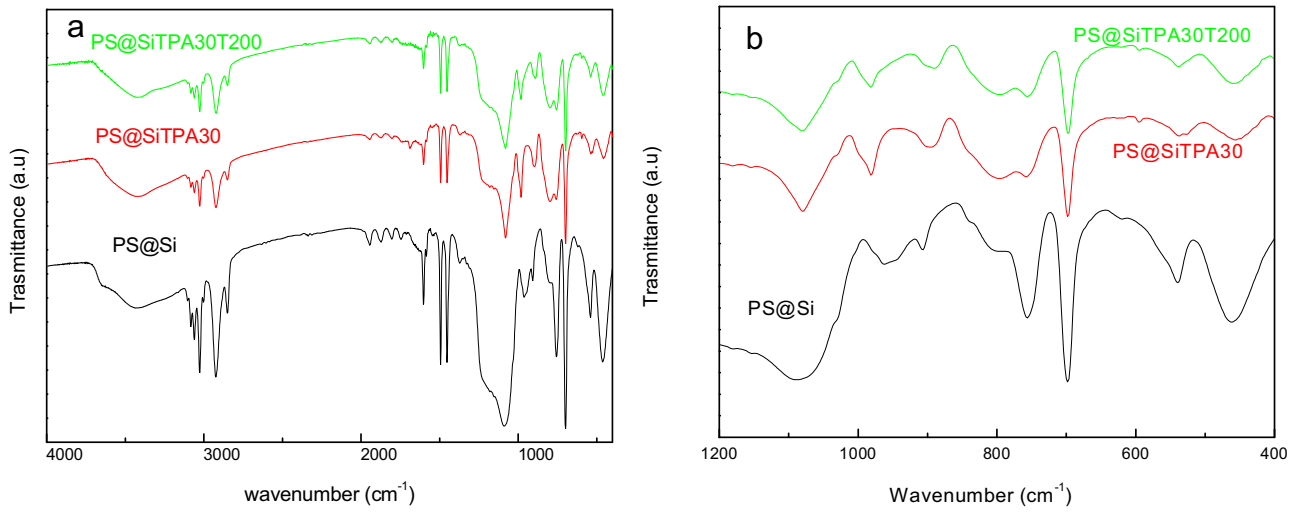

Fig. 3. FT-IR spectra of: a) PS@Si, PS@SiTPA30 and PS@SiTPA30T200 samples; b) the same solids in a wavenumber scale between 1200 and 400 cm^{-1}.

ore area (S_{micro}) estimated from the t-plot method [43], are listed in Table 1.

All the materials have a mean pore diameter greater than 2 nm, which corresponds to mesoporous materials, according to the IUPAC classification, and the micropore volume (V_{micro}) was negligible.

For the core-shell materials (PS@Si and PS@SiTPA30 samples), it was observed that TPA addition did not almost modify the surface area of the solid. When the solid was calcined at 200 °C after impregnation with the heteropolyacid (PS@SiTPA30T200 material), the S_{BET} value increased slightly due to a greater silica content in the material as a result of a higher Si/PS ratio. The solids containing

Table 1
Textural properties of the materials.

Sample	S_{BET} (m^2/g)	S_{micro} (m^2/g)	Vp (cm^3/g)	D_p (nm)
PS@Si	3	–	–	–
PS@SiTPA30	5	–	0.01	8.2
PS@SiTPA30T200	19	7	0.03	6.9
@SiT500	97	11	0.25	10.2
@SiT500TPA30	43	13	0.09	8.4
@SiT500TPA60	39	3	0.09	8.7
PS@SiTPA60	26	14	0.03	4.9
PS@SiTPA60T200	4	–	0.01	9.2

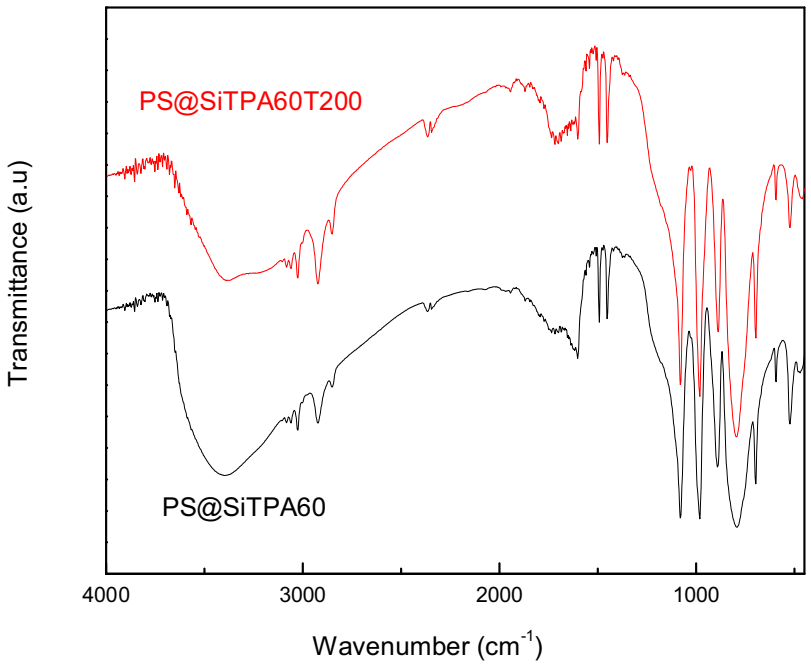

Fig. 4. FT-IR spectra of the solids impregnated with 60% TPA (w/w) before and after calcination at 200 °C.

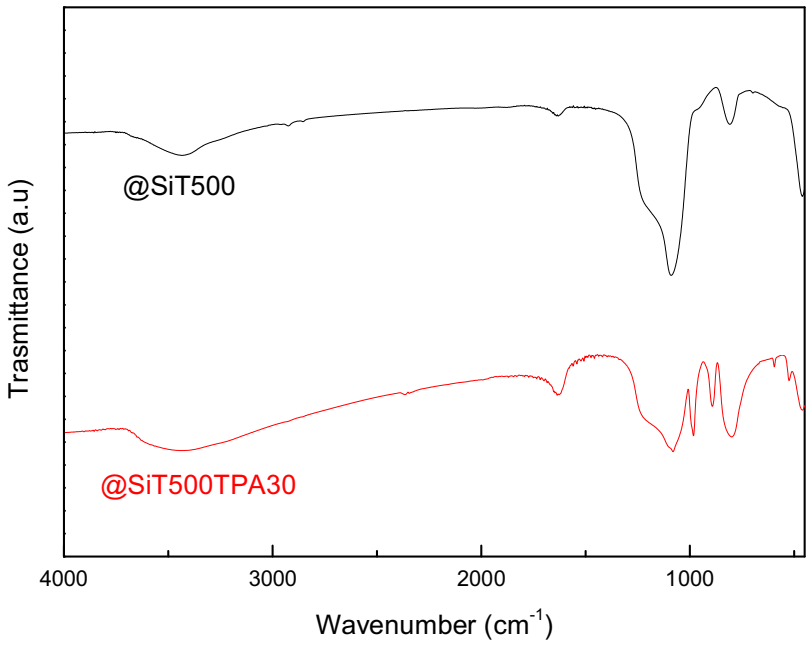

Fig. 5. FT-IR spectrum of the hollow silica spheres and the hollow spheres containing 30% TPA (w/w) obtained by impregnation with TPA solution.

a greater TPA amount (PS@SiTPA60 and PS@SiTPA60T200 samples) presented a similar behavior.

With regard to the @SiT500TPA30 and @SiT500TPA60 solids, i.e., the hollow spheres impregnated with TPA, the values of specific surface area were 43 and 39 m^2/g, respectively. As revealed by FT-IR spectroscopy, where the total loss of polystyrene in these samples was evident, and considering that the parent hollow spheres (@SiT500 sample) have an S_{BET} value of 97 m^2/g, higher than that of the samples considered, it can be concluded that there is a partial blockage of the pore mouths by the TPA anion, which decreased the mean pore size from 10.2 nm, corresponding to the bare hollow spheres, to 8.4 and 8.7 nm, obtained for the hollow spheres impregnated with TPA solutions.

The XRD patterns of the PS@Si sample and the materials containing 30% TPA (w/w) before (PS@SiTPA30 sample) and after calcination (PS@SiTPA30T200 sample) are shown in Fig. 6a. Peaks corresponding to crystalline phases, which are characteristic of the heteropolyacid, as well as a noncrystalline form interacting with the support, appear in the solids impregnated with TPA. Only a slight shift of the lines is observed when the material is calcined at 200 °C.

The material containing 60% TPA (w/w) (Fig. 6b) showed crystalline peaks assignable to the crystalline phase $H_3PW_{12}O_{40}{\cdot}23H_2O$ of tungstophosphoric acid. As in the previously presented solids, a slight shift of the peaks was observed when the material was cal-

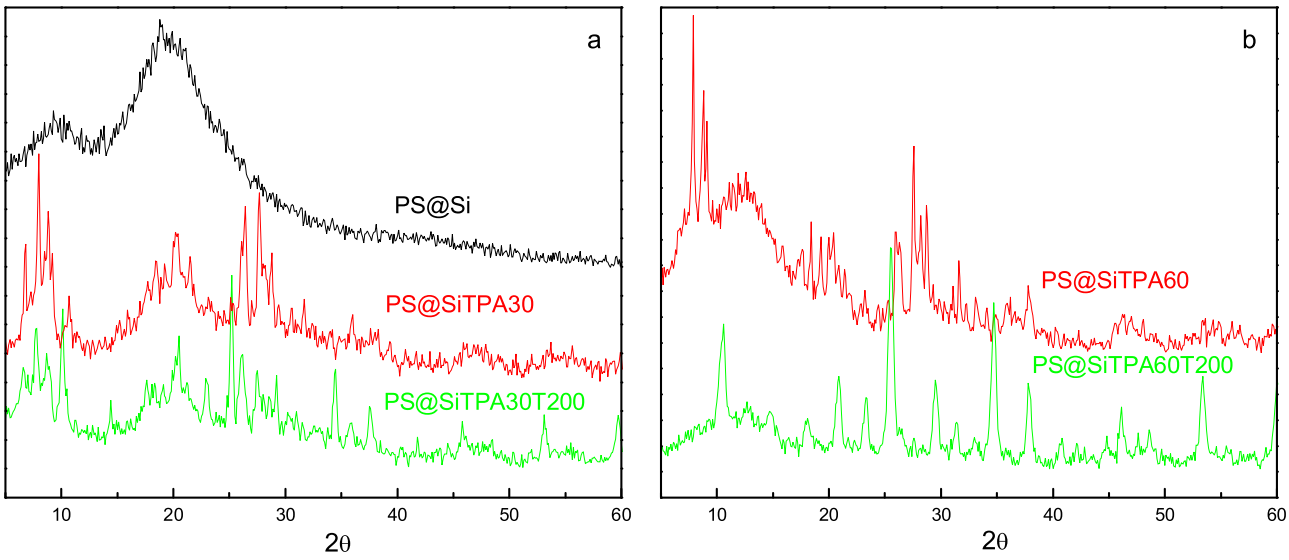

Fig. 6. XRD patterns of a) PS@Si, PS@SiTPA30 and PS@SiTPA30T200 samples, b) PS@SiTPA60 and PS@SiTPA60T200 samples.

cined at 200 °C, likely resulting from the phase transformation to the $H_3PW_{12}O_{40}{\cdot}6H_2O$ hydrate by loss of crystallization water.

A similar diffraction behavior was observed for the hollow silica spheres impregnated with TPA solution, containing 30% or 60% TPA (w/w) in the final solid.

The potentiometric titration with *n*-butylamine of the solids allows estimating the strength and the number of acid sites present in the solids. It is considered that the initial electrode potential (Ei) indicates the maximum strength of the acid sites, and the area under the curve accounts for the total number of acid sites that the titrated solid presents.

The strength of the acid sites can be classified according to the following scale: Ei > 100 mV (very strong sites), 0 < Ei < 100 mV (strong sites), −100 < Ei < 0 mV (weak sites), and Ei < 100 mV (very weak sites) [44].

From the potentiometric titration curves of the PS@SiTPA30 and PS@SiTPA30T200 solids, Ei values of 765 and 461 mV, respectively, were measured (Fig. 7a), so it could be established that the materials have very strong acid sites.

As observed, the potential decreased when the PS@SiTPA30 solid was thermally treated at 200 °C (PS@SiTPA30T200 sample), and also the number of acid sites diminished as the latter sample presented a lower area under the curve.

On the other hand, the titration curve of the support had a lower initial potential value (Ei = 127 mV) compared to those of the solids impregnated with TPA, due to the acidic characteristics of undegraded TPA.

Fig. 7b shows the curve corresponding to the PS@SiTPA60 solid. It is noted that this material has a similar acid strength to that of the PS@SiTPA30 solid and a higher number of acid sites. When the solid is calcined at 200 °C, the acid strength decreases, exhibiting a value of Ei = 525 mV (Fig. 7b).

The interaction between TPA and silica during impregnation can be considered as of electrostatic type due to proton transfer to the Si–OH groups. Then, by heat treatment after the impregnation, the elimination of a water molecule and the formation of a Si–O–W bond can occur, which could explain the decrease in the acidity values.

The hollow silica spheres were obtained after removal of the polystyrene core through calcination at 500 °C, as observed in the FT-IR spectra and SEM micrographs. Then, this material was impregnated with the TPA solutions, in order to prepare the @SiT500TPA30 and @SiT500TPA60 samples with a content of 30% or 60% TPA (w/w) in the solid, and the potentiometric titration was performed. These materials presented a very high acid strength, with values of Ei in the range 720–750 mV, similar to that of the PS@SiTPA30 and PS@SiTPA60 solids. The material with higher concentration (@SiT500TPA60 sample) displayed a slightly higher number of acid sites. This could be explained considering the migration of TPA into the hollow silica spheres, taking into account that the @SiT500 support has a Dp value of 10 nm and a TPA molecule has a diameter of 1 nm. As the driving force for diffusion into the hollow sphere is higher in the case of the solution with higher TPA concentration, this leads to an increase in the number of sites measurable by this technique.

3.2. *2,4,5-Triphenyl-1*H*-imidazole synthesis*

The trisubstituted imidazole synthesis was carried out as a multicomponent reaction, under solvent-free conditions, using benzyl, aldehyde and ammonium acetate as reagents, as shown in Scheme 1.

To obtain 2,4,5-triphenyl-1*H*-imidazole, the reactions were carried out with a benzyl: benzaldehyde:ammonium acetate molar ratio of 1:1:1.2, a catalyst amount of 1% mmol, at a reaction temperature of 130 °C, and a reaction time of 90 min, in the absence of solvent.

The product was characterized by ^{1}H NMR and ^{13}C NMR spectroscopy. The melting point (mp) of the solid was further determined. The results are in agreement with those reported in the literature and are listed below:

mp: 267–269 °C (lit. mp: 272–273 °C) [45]. ^{1}H NMR (500 MHz, DMSO-d_6): δ 12.70 (s, 1H); 8.09 (d, J = 7.8 Hz, 2H); 7.56–7.23 (m, 13H); ^{13}C NMR (125 MHz, DMSO-d_6): d 145.9, 137.5, 135.6, 131.5, 130.8, 129.1, 128.9, 128.7, 128.6, 128.3, 127.5, 126.9, 125.6.

The product yield values for the reactions carried out with the different catalysts are shown in Table 2. The yield obtained under the same reaction conditions without catalyst (catalyst-free) was rather low (19%). However, it can be considerably increased by using these acid catalysts.

Additionally, it is noteworthy to mention that in none of the experiments performed, by-products were formed, indicating that the catalysts are highly selective.

According to the performance values obtained, the catalyst that showed the best activity was the PS@SiTPA30 material, which exhibited 93% yield. The same catalyst, calcined at 200 °C

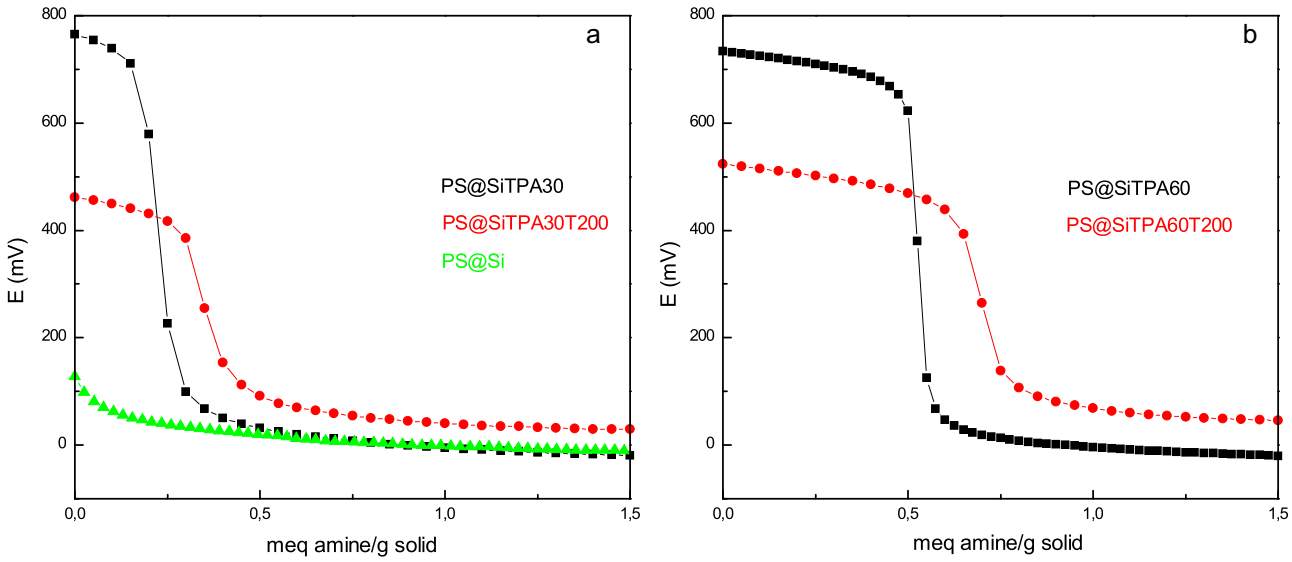

Fig. 7. Potentiometric titration curves of: a) PS@SiTPA30, PS@SiTPA30T200 and PS@Si solids, b) PS@SiTPA60 and PS@SiTPA60T200.

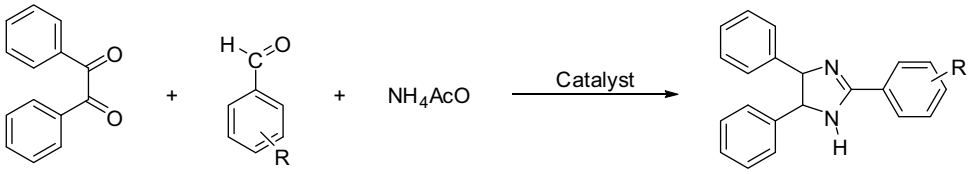

Scheme 1. Trisubstituted imidazole synthesis.

Table 2
2,4,5-Triphenyl-1*H*-imidazole synthesis employing the different TPA-based materials as catalysts.

Entry	Catalyst	Yield (%) to 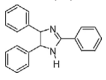
1	PS@SiTPA30	93
2	PS@SiTPA30T200	86
3	PS@SiTPA60	72
4	PS@SiTPA60T200	52
5	@SiT500TPA30	69
6	@SiT500TPA60	56

Reaction conditions: benzyl (1 mmol), aldehyde (1 mmol), ammonium acetate (1.2 mmol), catalyst (1% mmol) without solvent for 90 min at 130 °C.

(PS@SiTPA30T200 sample) afforded 86% yield, lower than that of the sample without calcination. The good catalytic activity of these materials has a nice correlation with their acidic characteristics. The characterization of the acidic behavior showed that the PS@SiTPA30 and PS@SiTPA30T200 solids have very strong acid sites, with especially high values of Ei (765 and 461 mV, respectively). It was also observed that the maximum acid strength and the number of acid sites decreased when the solid was calcined. For the materials containing 60% TPA (w/w) (PS@SiTPA60 and PS@SiTPA60T200 samples), the yield was significantly lower (52% and 49%, respectively) than those achieved using the aforementioned solids with a content of 30% TPA (w/w). The strength of acid sites in both series of catalysts was similar. However, in spite of the slightly higher number of acid sites, lower yields were obtained for the series with the highest TPA content. This may be attributed to the fact that the number and size of TPA crystals are significantly higher in the samples containing 60% TPA (w/w), according to the results obtained by XRD. These crystals have a low surface area and then, the number of accessible reactive protons is less than those achieved by supporting TPA in the form of small crystals or noncrystalline species. So, the lowest performance of the catalysts with higher TPA concentrations is because the reagents would be in contact with a lower number of acid sites.

With regard to the use of the hollow spheres impregnated with a TPA solution to obtain 30% TPA (w/w) (@ SiT500TPA30 sample) as catalyst, the yield obtained was 56%, while that obtained by using the hollow spheres containing 60% TPA (w/w) (@ SiT500TPA60 sample) was slightly higher (69%).

The acid strength of the sites present in the @SiT500TPA30 and @SiT500TPA60 materials is very high, since the Ei value exceeds 700 mV in both cases, and the latter sample presented a slightly higher number of acid sites. The lower product yield obtained in the synthesis of 2,4,5-triphenyl-1*H*-imidazole, when these catalysts are compared to core-shell materials, may be explained considering that a large percentage of TPA of the hollow solids is within the spheres and unable to act as catalyst during the synthesis.

The reusability of the catalysts was evaluated using the PS@SiTPA30 material. The results (Table 3) show that the yield slightly decreases for the first (90%) and second reuse (84%) and then, it remains constant. On the other hand, in all the cases the only product obtained was 2,4,5-triphenyl-1*H*-imidazole, showing that the selectivity remains unchanged.

3.3. *Synthesis of other trisubstituted imidazoles*

The trisubstituted imidazoles 2-(4-nitrophenyl)-4,5-diphenyl-1*H*-imidazole, 2-(4-methoxyphenyl)-4,5-diphenyl-1*H*-imidazole, and 2-(4-chlorophenyl)-4,5-diphenyl-1*H*-imidazole were prepared by using the catalyst PS@SiTPA30, which reached the best yield in the triphenyl-substituted imidazole synthesis, and working under the same reaction conditions though using the correspond-

Table 3
Synthesis of trisubstituted imidazoles using the PS@SiTPA30 solid as catalyst.

Entry	Product	Yield (%)
1	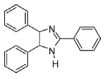	93
2	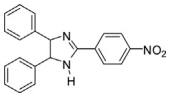	81
3	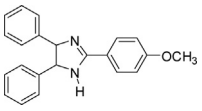	78
4	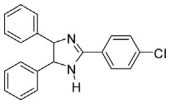	89

Reaction conditions: benzyl (1 mmol), aldehyde (1 mmol), ammonium acetate (1.2 mmol), catalyst (1% mmol) without solvent for 90 min at 130 °C.

ing aldehyde, i.e., 4-nitrobenzaldehyde, 4-methoxybenzaldehyde and 4-chlorobenzaldehyde, respectively.

The characterization of the products by ^{1}H NMR and ^{13}C NMR spectroscopy and melting point (mp) of the solid led to the following results.

2-(4-Nitrophenyl)-4,5-diphenyl-1H-imidazole: mp: 199–201 °C (lit. mp: 199–201 °C) [46]. ^{1}H NMR (500 MHz, DMSO-*d*6): δ 12.85 (s, 1H); 8.06–7.48 (m, 14H); ^{13}C NMR (125 MHz, DMSO-*d*6): d 148.8, 143.5, 131.5, 130.4, 129.8, 128.3, 127.7, 127.4, 126.8, 126.1, 125.3, 124.3, 122.3, 118.4.

2-(4-Methoxyphenyl)-4,5-diphenyl-1H-imidazole: mp: 220–223 °C (lit. mp: 226–228 °C) [47]. 1H NMR (500 MHz, DMSO-*d*6): δ 12.45 (s, 1H); 8.08 (d, J = 8.1 Hz, 2H); 7.52-7.32 (m, 10H); 7.07 (d, J = 8.4 Hz, 2H); 3.81 (s, 3H); ^{13}C NMR (125 MHz, DMSO-*d*6): d 159.4, 145.7, 128.3, 127.9, 126.8, 123.5, 114.4, 56.0.

2-(4-Chlorophenyl)-4,5-diphenyl-1H-imidazole: mp: 262–264 °C (lit. mp: 262–263 °C) [45]. ^{1}H NMR (500 MHz, DMSO-*d*6): δ 12.83 (s, 1H); 8.09 (d, J = 8.1 Hz, 2H); 7.57–7.25 (m, 12H); ^{13}C NMR (125 MHz, DMSO-*d*6): d 146.2, 130.3, 129.8, 129.2, 128.6, 127.4, 127.1, 126.5, 125.4, 125.2, 123.1, 116.1.

The product yield results for these compounds are listed in Table 3.

In all cases, high yields (>78%), without the presence of by-products (high selectivity), were obtained. We also performed the synthesis of trisubstituted imidazoles under the same conditions using the following aldehydes: 4-hydroxybenzaldehyde, 2-hydroxybenzaldehyde, 3-hydroxy-4-metoxybenzaldehyde, 4-methylbenzaldehyde, and 1-naphtaldehyde, obtaining high yields (90%, 84%, 81%, 87%, and 83%, respectively)

4. Conclusions

A heteropolyacid with Keggin structure, supported on core-shell type microspheres with polystyrene as core and silica as shell, and on hollow silica spheres, was used to replace traditional acid catalysts.

The polystyrene spheres coated with silica showed a smooth and uniform morphology, which was achieved by using tetraethylorthosilicate as a precursor of silica with a low amount of ammonium hydroxide as catalyst of the sol-gel reaction, and carefully controlling the condensation temperature.

The hollow silica spheres were obtained by calcination of the core-shell material at 500 °C, the core elimination being very effective because the spherical structure of the materials was maintained, and no rest of polystyrene was observed.

All the materials impregnated with tungstophosphoric acid (TPA) presented the undegraded tungstophosphate anion and contained very strong acid sites. In addition, these solids are mesoporous and presented crystalline TPA phases, together with a noncrystalline form interacting with the support

The behavior of the materials prepared was studied in the synthesis of trisubstituted imidazoles. It has been shown that the catalysts lead to a very high selectivity; the products were obtained without formation of secondary products in all cases. It was found that they showed a very good performance as acid catalysts for the synthesis of 2,4,5-triphenyl-1*H*-imidazole.

The core-shell material containing 30% TPA (w/w) showed the best performance compared to the rest of the materials prepared. This catalyst can be recovered and reused without appreciable loss of catalytic activity after three reuses. Its use as catalyst in the synthesis of other trisubstituted-imidazoles (2-(4-nitrophenyl)-4,5-diphenyl-1*H*-imidazole, 2-(4-methoxyphenyl)-4,5-diphenyl-1*H*-imidazole, and 2-(4-chlorophenyl)-4,5-diphenyl-1*H*-imidazole) also led to very good results.

In sum, materials that can be considered as sustainable catalysts were prepared, and they were used in a multicomponent reaction under free-solvent conditions with good results.

Acknowledgements

The authors thank the experimental contribution of E. Soto, G. Valle, M. Theiller, L. Osiglio, and the financial support of CONICET and UNLP. Consejo Nacional de Investigaciones Científicas y técnicas (CONICET PIP 628) and Universidad Nacional de la Plata (UNLP Project X638).

References

[1] M.V. Reddy, G.C.S. Reddy, Y.T. Jeong, Tetrahedron 68 (2012) 6820–6828.
[2] S. Maity, S. Pathak, A. Pramanik, Tetrahedron Lett. 54 (2013) 2528–2532.
[3] J.G. Lambardino, E.H. Wiseman, J. Med. Chem. 17 (1974) 1182.
[4] M. Misono, Chem. Commun. (2001) 1141–1152.
[5] J.W. Black, G.J. Durant, J.C. Emmett, C.R. Ganellin, Nature 248 (1974) 65–67.
[6] L. Wang, K.W. Woods, Q. Li, K.J. Barr, R.W. McCroskey, S.M. Hannick, L. Gherke, R.B. Credo, Y.H. Hui, K. Marsh, R. Warner, J.Y. Lee, N. Zielinsky-Mozng, D. Frost, S.H. Rosenberg, H.L. Sham, J. Med. Chem. 45 (2002) 1697–1711.
[7] Y.B. Nie, L. Wang, M.W. Ding, J. Org. Chem. 77 (2012) 696–700.
[8] J.A. Murry, Curr. Opin. Drug Discov. Dev. 6 (2003) 945–965.
[9] R. Kore, R. Srivastava, J. Mol. Catal. A: Chem. 376 (2013) 90–97.
[10] R. Kore, T.J. Dhilip Kumar, R. Srivastava, J. Mol. Catal. A: Chem. 360 (2012) 61–70.
[11] B. Radziszewski, Chem. Berich. 15 (1882) 1493–1496.
[12] F.R. Japp, H.H. Robinson, Chem. Berich. 15 (1882) 1268–1270.
[13] A. Shaabani, A. Rahmati, S. Naderi, Bioorg. Med. Chem. Lett. 15 (2005) 5553–5557.
[14] C. Kappe, Curr. Opin. Chem. Biol. 6 (2002) 314–320.
[15] R.K. Sharma, Shivani Sharma, Sriparna Dutta, Radek Zboril, Manoj B. Gawande, Green Chem. 17 (2015) 3207–3230.
[16] S. Rostamnia, N. Nouruzi, H. Xin, R. Luque, Catal. Sci. Technol. 5 (2015) 199–205.
[17] S. Wang, M. Zhang, W. Zhang, ACS Catal. 1 (2011) 207–211.
[18] M.B. Gawande, A. Goswami, T. Asefa, H. Guo, A.V. Biradar, D. Peng, R. Zboril, R.S. Varma, Chem. Soc. Rev. 44 (2015) 7540–7590.
[19] J. Huang, M. Zhang, J. Wang, X. Hu, R. Luque, F.L.Y. Lam, J. Mater. Chem. A 3 (2015) 789–796.
[20] F. Tang, L. Li, D. Chen, Adv. Mater. 24 (2012) 1504–1534.
[21] Y. Chen, H. Chen, Y. Sun, Y. Zheng, D. Zeng, F. Li, S. Zhang, X. Wang, K. Zhang, M. Ma, Q. He, L. Zhang, J. Shi, Angew. Chem. 123 (2011) 12713–12717.
[22] F. Caruso, Engineering of core–shell particles and hollow capsules, in: M. Rosoff (Ed.), Nano-surface Chemistry, Marcel Dekker, New York, USA, 2002, pp. 505–525.
[23] D.E. Lynch, Y. Nawaz, T. Bostrom, Lagmuir 21 (2005) 6572–6575.
[24] M.M. Titirici, A. Thomas, M. Antonietti, Adv. Funct. Mater. 17 (2007) 1010–1018.
[25] Z.Y. Zhong, Y.D. Yin, B. Gates, Y.N. Xia, Adv. Mater. 12 (2000) 206–209.
[26] F. Caruso, R.A. Caruso, H. Möhwald, Science 282 (1998) 1111–1114.
[27] D. Walsh, B. Lebeau, S. Mann, Adv. Mater. 11 (1999) 324–328.

[28] C.I. Zoldesi, A. Imhof, Adv. Mater. 17 (2005) 924–928.
[29] Q. Peng, Y.J. Dong, Y.D. Li, Angew. Chem. Int. Ed. 42 (2003) 3027–3030.
[30] Q.H. Yang, D.F. Han, H.Q. Yang, C. Li, Chem. Asian J. 3 (2008) 1214.
[31] W. Stöber, A. Fink, E. Bohn, J. Colloid Interface Sci. 26 (1968) 62–69.
[32] M.S. Tsai, M.J. Li, J. Non-cryst. Solids 352 (2006) 2829–2833.
[33] S. Zhang, L. Xu, H. Liu, Y. Zhao, Q. Wang, Z. Yu, Z. Liu, Mater. Lett. 63 (2009) 258–259.
[34] M. Gorsd, M.N. Blanco, L.R. Pizzio, Procedia Mater. Sci. 1 (2012) 432–438.
[35] W. Stöber, A. Fink, E.J. Bohn, J. Colloid Interface Sci. 26 (1968) 62–69.
[36] E. Rafiee, H. Mahdavi, M. Joshaghani, Mol. Divers. 15 (2011) 125–134.
[37] M. Gorsd, L.R. Pizzio, M.N. Blanco, Synthesis and characterization of hollow silica spheres, Procedia Mater. Sci. 8 (2015) 567–576.
[38] The Aldrich Library of Infrared Spectra, in: C.J. Pouchert (Ed.), Edición III, Aldrich Chemical Co., 1981.
[39] L.R. Pizzio, P.G. Vázquez, C.V. Cáceres, M.N. Blanco, Appl. Catal. A: Gen. 256 (2003) 125–139.
[40] C. Rocchiccioli-Deltcheff, R. Thouvenot, R. Franck, Spectrochim. Acta A 32 (1976) 587.
[41] L.R. Pizzio, M.N. Blanco, Appl. Catal. A: Gen. 255 (2003) 265–277.
[42] D.C.L. Vasconcelos, W.R. Campos, V. Vasconcelos, W.L. Vasconcelos, Mater. Sci. Eng. A 334 (2002) 53–58.
[43] R. Sh Mikhail, S. Brunauer, E.E. Bodor, J. Colloid Interface Sci. 26 (1968) 45.
[44] L. Pizzio, P. Vázquez, C. Cáceres, M. Blanco, Catal. Lett. 77 (2001) 233–239.
[45] M. Kidwai, P. Mothsra, V. Bansal, R.K. Somvanshi, A.S. Ethayathulla, S. Dey, T.P. Singh, J. Mol. Catal. A: Chem. 265 (2007) 177–182.
[46] S. Samai, G.C. Nandi, P. Singh, M.S. Singh, Tetrahedron 65 (2009) 10155–10161.
[47] M.M. Heravi, K. Bakhtiari, H.A. Oskooie, S. Taheri, J. Mol. Catal. A: Chem. 263 (2007) 279–281.